Modeling and fast simulation of RF-MEMS switches within standard IC design frameworks

M. Niessner, G. Schrag and G. Wachutka
Institute for Physics of Electrotechnology
Munich University of Technology
Munich, Germany
niessner@tep.ei.tum.de

J. Iannacci
MEMS Research Unit
Fondazione Bruno Kessler (FBK)
Povo di Trento, Italy
iannacci@fbk.eu

***Abstract*— We present a macromodel of an electrostatically actuated and viscously damped ohmic contact RF-MEMS switch suitable for direct implementation in standard IC design frameworks. The physics-based and multi-energy domain coupled model is systematically derived on the basis of a hierarchical modeling approach. The very good agreement with measurements proves the capability of the model to predict the behavior of the RF-MEMS switch. Especially effects due to the nonlinear coupling of the different energy domains are correctly reproduced. The accurate reproduction of heavily contact-related situations within acceptable computing time is identified as an issue for future research.**

I. INTRODUCTION

A key prerequisite for the routine use of radio frequency microelectromechanical (RF-MEMS) switches as standard circuit elements is the availability of computationally efficient, but yet physics-based and, thus, predictive models, which correctly describe the switching behavior of micromechanical switches. Furthermore, these models should use a framework that is easy to use for RF circuit designers and that allows for an integrated design of semiconductor-based RF circuits with MEMS hybridization. The simulation of the switching behavior, i.e. of the pull-in and pull-out transients of RF-MEMS devices, is, however, a challenging task because it demands the consideration of multiple energy domains and their nonlinear interactions.

The finite element method (FEM) is efficient when a single physical energy domain is the sole focus of the optimization, but becomes computationally expensive and difficult to handle when multiple energy domains with potentially large mesh deformations have to be coupled and analyzed together. Furthermore, RF circuit designers are usually not trained to perform multi-energy domain coupled simulations with FEM-based simulation tools. The preferred method for enabling the fast simulation of pull-in/-out transients is therefore the use of multi-energy domain coupled macromodels that can be simulated within standard integrated circuit (IC) design frameworks.

In this paper, a physics-based macromodel of an RF-MEMS switch (cp. fig. 1), which can be directly used for co-simulation with electronic circuits in a standard IC design framework, is derived and evaluated w.r.t. measurements performed with a Wyko NT1100 DMEMS white light interferometer (WLI) from Veeco.

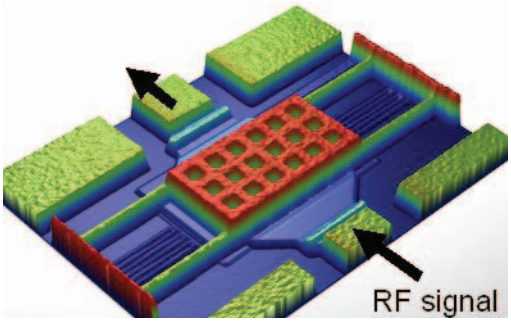

Figure 1. Measured (WLI) 3D profile of the RF switch without bias.

II. RF-MEMS SWITCH USED FOR EVALUATION

The electrostatically actuated and viscously damped ohmic contact RF-MEMS switch analyzed in this work (cp. fig. 1) is fabricated at Fondazione Bruno Kessler (FBK) [1]. The RF-MEMS technology available at FBK relies on a surface micromachining process based on gold. The switch consists of a movable gold membrane suspended above a fixed ground electrode through four straight beams. The membrane on the scale of 140µm x 260µm x 5µm is perforated with square holes having a side length of 20µm. The fixed ground electrode acts as actuation electrode of the switch and consists of several lateral fingers that are connected in parallel (cp. fig. 2).

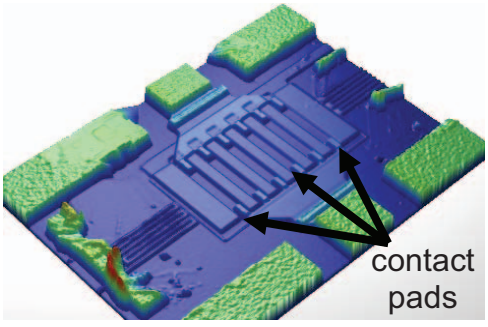

Figure 2. Measured (WLI) profile of the electrodes and the 12 elevated contact pads. The membrane was removed for this measurement.

978-1-4244-7700-5/10/$26.00 ©2010 IEEE

By applying a voltage, the suspended membrane can be pulled towards the ground electrode. As the voltage is increased, pull-in occurs and the membrane collapses onto 12 elevated contact pads. In this way, an ohmic contact is closed and RF signals are able to pass through the device. The gap height g_0 between the membrane and the contact pads is 1.4µm. The gap height between the membrane and the fixed ground electrode amounts to 3µm.

III. MODELING

The macromodel of the switch is derived on the basis of the hierarchical modeling approach as reported in [2]. The approach allows to combine flux-conserving reduced-order and compact modeling techniques that derive both lumped and distributed macromodels in terms of conjugated variables (”across”- and ”through”-variables). As the approach employs generalized Kirchhoffian network theory as a theoretical framework for the coupling of multiple energy domains, Kirchhoff’s laws govern the exchange of all physical quantities between the macromodels.

The simulation of pull-in/-out transients demands the formulation and coupling of four distinct submodels: a mechanical submodel of the suspended membrane, an electrostatic one describing the electrostatic field and attracting forces between the membrane and the fixed ground electrode, a fluidic one of the viscous damping forces acting on the moving membrane, and a model of the mechanical contact between the membrane and the contact pads. The following sections briefly outline the different techniques employed for submodel generation and the four resulting submodels.

A. Mechanical submodel: suspended membrane

The modal superposition technique [3] is used to derive a physics-based reduced-order model of the suspended membrane. The respective eigenmode shapes and frequencies were calculated in the FEM simulation tool ANSYS^{TM}. Fabrication-induced residual stresses are taken into account by adjusting the fundamental eigenfrequency of the FEM model to the measured one of 14.7kHz. The modeling procedure results in a macromodel with only one second-order differential equation per included eigenmode:

$$\ddot{q}_i + \omega_i^2 q_i = \overline{\theta}_i^T \overline{F}_{ext} \tag{1}$$

Here, q_i and ω_i denote the amplitude and the frequency of the i-th eigenmode. $\overline{\theta}_i$ denotes the vector of the discretized shape of the i-th eigenmode. $\overline{\theta}_i$ is normalized w.r.t. the mass matrix. $\overline{F}_{ext}$ denotes the vector of the external forces acting on the membrane, i.e. in case of the switch, electrostatic, viscous damping and contact forces.

B. Electric submodel: electrostatic actuation

The submodel of the electrostatic forces exerted by the ground electrode is derived in two steps. First, the electrostatic energy E_k stored between each k-th finger and the membrane is determined in terms of the modal amplitudes. Second, Lagrangian energy functionals $L_{k,i}$ are calculated for each eigenmode i :

$$L_{estat,k,i}(\overline{q}) = \frac{\partial E_k(\overline{q})}{\partial q_i} = \frac{1}{2}\frac{\partial C_k(\overline{q})}{\partial q_i}(V_k)^2 \tag{2}$$

Here, $\overline{q}$ denotes the vector of modal amplitudes and $C_k(\overline{q})$ the capacitance of the k-th finger configuration. V_k is the respective voltage applied. The physical character of the Lagrangian energy functionals is that of a mechanical ”through”-quantity, i.e. the functionals can be directly added to the respective eigenmode equation (eq. 1). Since the seven fingers of the electrode can be considered as electrostatically decoupled, but with a common bias V_b, the electromechanically coupled model equations read:

$$\ddot{q}_i + \omega_i^2 q_i = \frac{V_b^2}{2}\sum_{k=1}^{7}\frac{\partial C_k(\overline{q})}{\partial q_i} + \overline{\theta}_i^T \overline{F}_{ext} \tag{3}$$

C. Fluidic submodel: viscous damping forces

The mixed-level approach as presented in [4] is used for the modeling of the viscous damping forces exerted by the ambient atmosphere, i.e. the Reynolds equation is combined with physics-based fluidic resistances that account for the pressure drop at the perforations and at the outer boundary. The so enhanced Reynolds equation is evaluated in a distributed fluidic Kirchhoffian network. Consequently, this approach does not result in a lumped model, but in a distributed finite network model with a larger number of degrees of freedom. However, the advantage of this physics-based description is that it is tailored to the topography of the real membrane with all its perforations and locally varying gap heights and has therefore the capability to predict the damping forces quite accurately. The viscous damping forces $F_{d,n}$ at an ambient pressure p_0 are calculated by multiplying the nodal pressures P_n with the corresponding nodal areas A_n:

$$F_{d,n}(\overline{q}, \dot{\overline{q}}, p_0) = A_n P_n(\overline{q}, \dot{\overline{q}}, p_0) \tag{4}$$

D. Contact submodel: mechanical contact

The submodel for the mechanical contact is given by contact forces $F_{c,m,i}$ at the respective nodes m above the contact pads. Each nodal force is modeled by a dissipative term that accounts for the losses during contact and a contact stiffness that accounts for the deformation stiffness of the contact pads:

$$F_{c,m,i}(\overline{q}, \dot{q}_i) = d_{contact,i}\dot{q}_i + k_{contact}(h_n(\overline{q}) + g_0) \tag{5}$$

Here, $\dot{q}_i$ denotes the velocity of the i-th mode, $h_m(\overline{q}, t)$ the local displacement at the m-th node and the parameters $\boldsymbol{d}_{contact,i}$ and $\boldsymbol{k}_{contact}$ denote the contact damping and stiffness. The force is only present if the following condition is met:

$$h_m(\overline{q}) + g_0 < 0 \tag{6}$$

E. Fully coupled macromodel

The viscous damping forces and the nodal contact forces are coupled with the electromechanical eigenmode equations (eq. 3) through the vector of external forces:

$$F_{ext,n,i}(\bar{q},\dot{\bar{q}},p_0) = F_{d,n}(\bar{q},\dot{\bar{q}},p_0) + F_{c,n,i}(\bar{q},\dot{q}_i) \quad (7)$$

The contact forces are only present at nodes above contact pads and elsewhere equal to zero. Consequently, the electromechanical-fluidic coupled eigenmode equations including contact read:

$$\ddot{q}_i + \omega_i^2 q_i = \frac{V_b^2}{2}\sum_{k=1}^{7}\frac{\partial C_k(\bar{q})}{\partial q_i} + \bar{\theta}_i^T \bar{F}_{ext,i}(\bar{q},\dot{\bar{q}},p_0) \quad (8)$$

F. AUTOMATIC MODEL GENERATION

The practical use of the above-described approach is strongly facilitated by a modeling toolbox developed in MATLAB™. The toolbox enables the automated generation of mixed-level approach based macromodels, starting from a given FEM model in ANSYS™ and the respective eigenmodes (cp. fig. 3). Models on different descriptive levels are already implemented and can be selected as modules according to the specific requirements. In order to automatically generate the fluidic mixed-level model, the toolbox applies a set of self-developed algorithms to the discretized geometry of the device. The output of the toolbox is a fully coupled model coded in a hardware description language (HDL) ready for co-simulation with electronic circuits in a standard IC design framework.

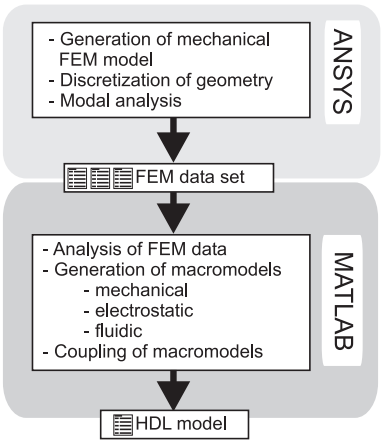

Figure 3. Workflow for the generation of macromodels employing a MATLAB™-based modeling toolbox.

IV. RESULTS

The evaluation of the macromodel w.r.t. measurements is performed in four steps. First, the measured and the simulated quasi-static pull-in/-out characteristics of the switch are compared in order to assess the electric and mechanical submodels. Second, the measured transient response of the switch to an actuation with two voltage step functions is used to benchmark the coupled fluidic, electric and mechanical submodels. Third, the validity of the fluidic submodel at varying ambient pressure conditions is tested. Fourth, the measured and the simulated pull-in/-out transients of the switch are used to evaluate the complete macromodel.

In order to minimize the effect of dielectric charging [5] in the measurement of the quasi-static pull-in/-out characteristics, the switch was actuated with a 70V pp (peak-to-peak) zero mean value triangular voltage waveform at 20Hz. The pull-in of the membrane occurs at 30.5V and the release at 24V (cp. Fig. 4). The same actuation was applied in the macromodel-based simulation. Figure 4 shows a comparison of the measured data and the simulated results. In case of the pull-in characteristic, simulation and measurement show a very good agreement. This proves that the techniques employed for the derivation of reduced-order and compact models of the mechanical and electrostatic problems were able to generate submodels that accurately describe the physics of this experiment. On the other hand, the simulation calculates an incorrect release voltage. This is due to the fact that no adhesion forces, no dielectric charging or other contact-related phenomena were yet considered in the contact submodel. Only the electric hysteresis is accounted for.

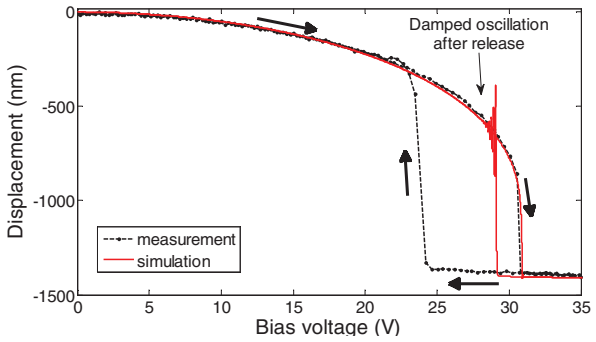

Figure 4. Quasi-static measured and simulated pull-in/-out characteristics of the membrane as caused by a bias of triangular waveform Due to the particular experimental setup, the damped oscillation after release is not captured by the measurement. Only the first half of the cycle with positive voltages rising from 0 to 35V and decrasing from 35V to 0V is shown.

In order to evaluate the coupled fluidic, electric and mechanical submodels, the switch was actuated with a voltage of rectangular waveform of 25V pp at 500Hz and with a 50% duty-cycle. In this experiment, the electrostatic forces attract the membrane during the first half of the cycle, so that the latter settles after a damped oscillation at a displacement of about 12% of the gap height (cp. fig. 5). In the second half of the cycle, the electrostatic forces are no longer present and the membrane returns, after a damped oscillation, to its initial position. The very good agreement between measured and simulated data allows for important conclusions: the good agreement in the second half of the cycle proves that the fluidic mixed-level model calculates accurately the viscous damping forces that are acting on the released membrane. The good agreement in the first half of the cycle proves furthermore, that the nonlinear coupling between the three active submodels is correctly accounted for. The electrostatic forces effectively decrease the stiffness of the electromechanically coupled system (eq. 3), an effect also known as spring softening. The macromodel accurately reproduces this effect: the resonance frequency in the first half of the cycle is indeed 12.2kHz and not 14.7kHz as in the second one. The fluidic model also correctly calculates the increased damping in the first half of the cycle. The damping is stronger in the first half of the cycle because the gap height is decreased by, as stated earlier, 12%.

The limits of the fluidic mixed-level submodel is evaluated by performing transient measurements at varying ambient pressure conditions and by calculating the rate of decay δ as a measure of viscous damping. The fluidic submodel uses correction factors to account for rarefaction effects [7] and shows good agreement down to ambient

pressures of 200hPa (1hPa=1mbar). For lower pressures, the fluidic submodel overestimates the viscous damping forces.

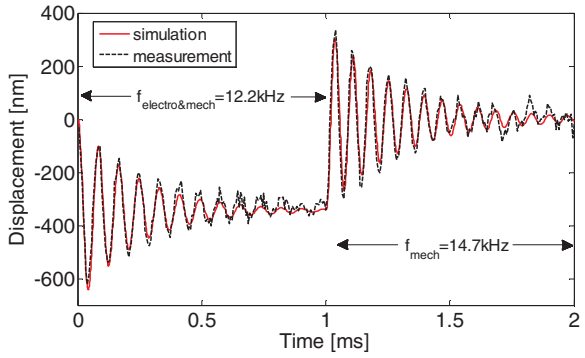

Figure 5. Measured and simulated response of the membrane. Actuation: rectangular voltage waveform at 500Hz and of the amplitudes 26V (on) and 0V (off). 50% duty-cyle. Ambient pressure: 600hPa.

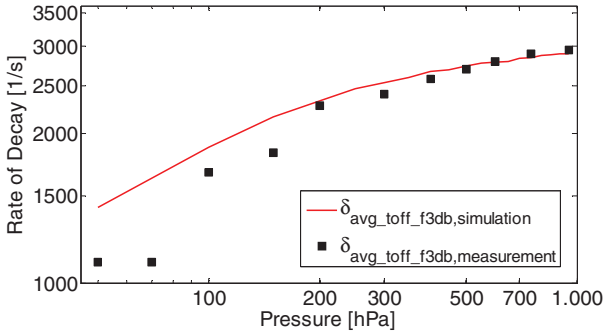

Figure 6. Comparison of the simulated and measured rates of decay δ. The plot shows an average of the rates of decay calculated from the frequency spectrum ("f3db") and from the damped oscillation whilst the off-period ("toff", cp. fig 5., t=1..2ms).

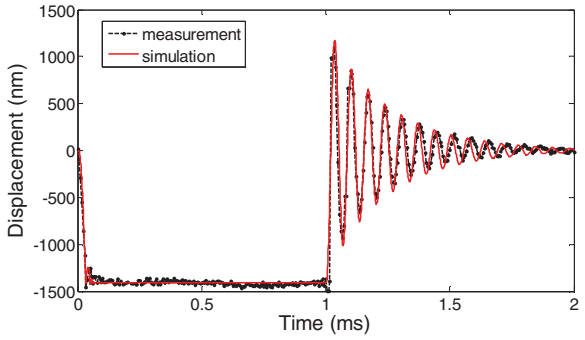

Figure 7. Measured and simulated transient pull-in/-out of the membrane. Actuation: rectangular voltage waveform at 500Hz and of the amplitudes 36V (on) and 0V (off). 50% duty-cycle. Ambient pressure: 960hPa.

In order to measure the pull-in and pull-out transients of the membrane, the switch was actuated with a rectangular voltage waveform of 36V pp at 500Hz and with a 50% duty-cycle. A comparison of the measured and simulated data (cp fig. 7) shows that the macromodel reproduces the pull-out transient of the membrane with acceptable accuracy.

On the other hand, the pull-in transient of the membrane is, after the first impact of the membrane, only crudely reproduced. This is due to the fact that the contact submodel does not yet cover the correct physics during impacts [6].

V. CONCLUSION

The proposed multi-energy domain coupled macromodel shows very good agreement with the measured quasi-static pull-in characteristic, with the non-contact transient measurements for ambient pressures down to 200hPa and acceptable agreement with the pull-out transient after contact. However, the macromodel fails in reproducing the measured quasi-static pull-out characteristic and the measured pull-in transient. Obviously, the macromodel is not yet able to give accurate and predictive results in strong contact-related situations. This is due to the simplicity of the contact submodel (eq. 5). Future research will focus on this issue. Contact-related effects like dielectric charging, adhesion forces [8], stiction and the physics during the impact of the membrane [6] need to be considered.

The general question is, however, what degree of accuracy a macromodel of an RF-MEMS switch is supposed to deliver. The more detailed the contact model gets, the higher the computational expense will be. If the computing time is to be kept low, a simple contact model, as the one used in this paper, which is carefully calibrated by experiments and combined with a circuit model of dielectric charging [5], might represent the best solution of the trade-off between simulation time and accuracy.

References

[1] J. Iannacci, F. Giacomozzi, S. Colpo, B. Margesin and M. Bartek, "A General Purpose Reconfigurable MEMS-Based Attenuator for Radio Frequency and Microwave Applications", in Conf. Proc. of EUROCON, 2009, pp: 1201-1209.

[2] G. Schrag, R. Khaliliyulin, M. Niessner, and G. Wachutka, "Hierarchical Modeling Approach for Full-System Design and control of Microelectromechanical Systems," in Conf. Proc. of Eurosensors XXII, 2008, pp. 528-531.

[3] L. Gabbay, J. Mehner, and S. Senturia, "Computer-aided generation of reducedorder dynamic macromodels - I: Geometrically linear motion," J. Microelectromechanical Systems, vol. 9, 2000, pp. 262–269.

[4] Schrag G., and Wachutka G., "Physically based modeling of squeeze film damping by mixed-level system simulation," Sensors and Actuators A, vol. 97-98; 2002 , pp. 193–200.

[5] R. Marcelli, et al., "Reliability of RF MEMS switches due to charging effects and their circuital modelling," J. Microsystem Technologies, vol. 16, no. 7, 2010, pp. 1111-1118.

[6] M. Niessner, J. Iannacci, A. Peller, G. Schrag, and G. Wachutka, "Macromodel-based simulation and measurement of the dynamic pull-in of viscously damped RF-MEMS switches," in Conf. Proc. of Eurosensors XXIV, 2010, in press.

[7] M. Niessner, G. Schrag, G. Wachutka, J. Iannacci, T. Reutter and H. Mulatz, "Non-linear model for the simulation of viscously damped RF-MEMS switches at varying ambient pressure conditions," in Conf. Proc. of Eurosensors XXIII, 2010, pp. 618-621.

[8] Z.Guo, N. McGruer, and G. Adams, "Modeling, simulation and measurement of the dynamic performance of an ohmic contact, electrostatically actuated RF MEMS swtich," in J. Micromechanics and Microengineering, vol. 17, 2007, pp. 1899-1909.